Onset of thermally driven self-motion of a current filament in a bistable semiconductor structure

Pavel Rodin*
Ioffe Physicotechnical Insitute of Russian Academy of Sciences, Politechnicheskaya 26, 194021 St. Petersburg, Russia
(Received 7 July 2004; published 10 February 2005)

We perform an analytical investigation of the bifurcation from static to traveling current density filaments in a bistable semiconductor structure with S-shaped current-voltage characteristic. Joule self-heating of a semiconductor structure and the effect of temperature on electron transport are consistently taken into account in the framework of a generic reaction–diffusion model with global coupling. It is shown that the self-heating is capable of inducing translation instability which leads to spontaneous onset of lateral self-motion of the filament along the structure. This may occur in a wide class of semiconductor structures whose bistability is caused by impact ionization due to the negative effect of temperature on the impact ionization rate. The increment of the translation mode and the instability threshold are determined analytically.

DOI: 10.1103/PhysRevB.71.085309 PACS number(s): 72.20.Ht, 05.70.Ln, 85.30.−z

I. INTRODUCTION

Current density filament in a bistable semiconductor structure with S-shaped current–voltage characteristic is a high current density domain embedded in a low current density environment.[1–9] Typically filaments appear spontaneously due to spatial instability of the uniform current flow when the average current density corresponds to the falling branch of the current–voltage characteristic.[2] A single filament survives after the transient (the-winner-takes-all principle) whereas multifilamentary states are unstable.[3–9] A static current filament may undergo further bifurcations related to temporal and spatial instabilities.[10–22] Spontaneous onset of the lateral movement is an example of such a bifurcation which has been recently studied both experimentally and theoretically.[17–22] This effect is of significant practical importance because the filament motion delocalizes the Joule heating of a semiconductor structure operated in the current filamentation regime, and thus dramatically reduces the probability of thermal failure.[18–21] Traveling current density filaments bear deep similarities to other traveling spots in active media,[23–28] in particular, to traveling wave segments in feedback controlled light sensitive Belousov–Zabotinsky reaction.[29,30]

The latest experimental observations of moving filaments[17,18,20,21] have been made using a recently developed interferometric mapping technique.[17] Experiments show that in a device with a stripelike geometry the filament travels in a solitonlike manner with a constant velocity $\sim 1\ \mathrm{m/s}$ and reflects from the device boundaries. Both measurements and full-scale numerical simulations of the transport processes suggest that the filament motion is thermally driven and related to the Joule self-heating.[17,18,21] Thermally driven self-motion is possible due to the negative effect of temperature on the impact ionization rate[31,32] and may occur in a wide class of semiconductor structures whose bistability is caused by impact ionization.[15,22] The temperature acts as an inhibitor which provokes translation instability of a steady filament and causes its self-sustained motion toward a cooler region.[15,22]

In this paper we present an analytical investigation of the translation instability which occurs at the onset of thermally driven filament motion. Using a recently suggested three-component reaction–diffusion model for current filamentation in presence of the Joule self-heating,[22] we perform a stability analysis of a static filament. We show that the translation invariance of a static filament in a large structure breaks in presence of the self-heating. This occurs with increase of the thermal relaxation time which depends on the heat capacity of the semiconductor structure and the efficiency of the external cooling. The instability threshold decreases when the effect of temperature on the vertical transport becomes stronger and increases with heat diffusion coefficient.

II. THE MODEL

Current filamentation in bistable semiconductors can be described by a two-component activator–inhibitor model which consists of a nonlinear reaction–diffusion equation, accounting for the internal activator dynamics in a bistable semiconductor, and an integrodifferential equation, accounting for the applied voltage. This model, originally developed for bulk semiconductors with so-called overheating instability[3,4] and layered semiconductor structures,[5–7] proved to be efficient for a wide class of bistable semiconductors with various mechanims of bistability (see Ref. 33, and references therein). We refer to Refs. 34–36 for comprehensive general formulation of this model.

To decribe the thermally driven motion of a current density filament, the effect of temperature T on the cathode–anode transport and the heat dynamics in the structure should be additionally taken into account. The respective extension of the conventional two-component model[34–36] has been recently suggested in Ref. 22:

$$\frac{\partial a}{\partial t} = \nabla_{\perp}[D_a(a)\nabla_{\perp} a] + f(a,u,T), \tag{1}$$

$$\tau_T \frac{\partial T}{\partial t} = \ell_T^2 \Delta_{\perp} T + (Ju/\gamma + T_{\mathrm{ext}} - T), \tag{2}$$

 ©2005 The American Physical Society

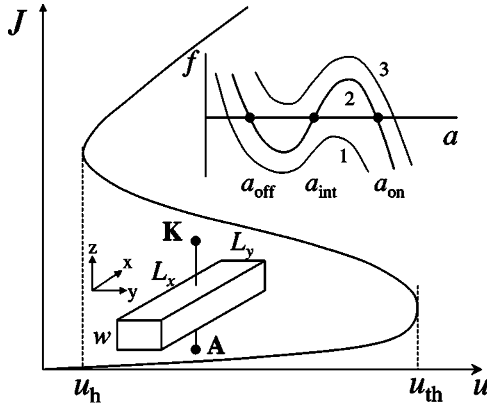

FIG. 1. S-shaped current–voltage characteristic $J(u)$ of a bistable semiconductor structure. The upper inset shows the local kinetic function $f(a,u)$ for $u<u_h$, $u_h<u<u_{th}$, and $u>u_{th}$ (curves 1, 2, and 3, respectively), where u_h and u_{th} are the hold and the threshold voltages at the edges of the bistability range. For $u_h<u<u_{th}$ the local kinetic function has three zeros corresponding the off, intermediate, and on branches of the current-voltage characterisics, respectively. The lower inset sketches the rectangular semiconductor structure elongated along the x axis.

$$\tau_u \frac{du}{dt} = U_0 - u - R \int_S J(a,u) dx dy, \quad \tau_u \equiv RC. \tag{3}$$

Here a acts as an activator, u and T as inhibitors.

Equations (1) and (3) are the same as in the conventional two-component model.[34,35] The variable $a(x,y,t)$ characterizes the internal state of the device and $u(t)$ is the voltage over the device. The local kinetic function f and the $J(a,u)$ dependence contain the information about the vertical electron transport in the cathode–anode direction and together determine the S-shaped local current–voltage characteristic (Fig. 1). The function $f(a,u)$ has three zeros corresponding to the off, intermediate and on states, respectively, when the voltage u is within the bistability range $[u_h, u_{th}]$ (the upper inset in Fig. 1). The diffusion coefficient $D_a(a)$ characterizes lateral [along the (x,y) plane] coupling in the spatially extended semiconductor structure. Equation (3) is a Kirchhoff's equation for the external circuit. R is the load resitance switched in series with the semiconductor structure, U_0 is the total applied voltage, C is the effective capacitance of the sample and the circuit, and S is the device area of the structure cross section. In the following we consider the current-controlled regime.

Equation (2) describes the heat dynamics in the structure. Similar to the variable a, the temperature $T(x,y,t)$ depends only on the lateral coordinates x and y. T_{ext} is the temperature of the external cooling reservoir, γ is heat transfer coefficient, the termal relaxation time τ_T and diffusion length ℓ_T are given by

$$\tau_T \equiv c\rho w/\gamma, \quad \ell_T \equiv \kappa w/\gamma, \tag{4}$$

where c, ρ, and κ are specific heat, density, and heat conductivity of the semiconductor material, respectively, and w is the device thickness in the cathode–anode direction.

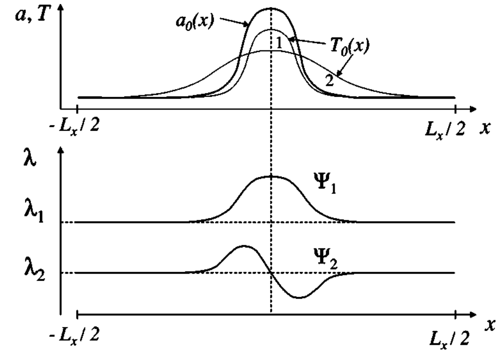

FIG. 2. Profile $a_0(x)$ of the activator and the temperature profile $T_0(x)$ in a steady filament (the upper panel). The current denisity profile $J[a_0(x),u]$ is quailitatively the same as $a_0(x)$. The temperature profile $T_0(x)$ is sketched for weak ($\ell_T \ll \ell_a$, curve 1) and strong ($\ell_T \gg \ell_a$, curve 2) heat diffusion. Note that in our analysis L_x is much larger than the filament width. The lower panel shows two first eigenfunctions Ψ_1 and Ψ_2 of the operator $\hat{H}_a$ and their eigenvalues λ_1, λ_2. Ψ_1 and Ψ_2 are eigenmodes of the steady filament in a voltage controlled regime and correspond to expansion (shrinking) and translation of the filament, respectively. In the isotheramal case $\lambda_2=0$ and $\Psi_2 \equiv \Psi_G \sim a_0'$.

The continuity equation (1) is coupled to the heat equation (2) via the temperature dependence of the local kinetic function $f(a,u,T)$. Since the heating suppresses impact ionization, the effect of temperature on the vertical transport is negative and $\partial_T f < 0$.[37] The direct dependence of the current density J on T is neglected.

The characteristic size of a filament wall is $\ell_a \equiv \sqrt{D_a/\partial_a f}$.[34,35] Parameters ℓ_a and ℓ_T are diffusion lengths of the activator and inhibitor, respectively. For simplicity, in the following we take $D_a(a)=$const. Next, we take into account only one lateral dimension x, assuming that due to the stripe geometry of the semiconductor structure ($L_x \gg \ell_a \gg L_y$) the current density distribution is uniform along the y direction (the lower inset in Fig. 1). We also assume that the filament is located far from the edges of the stripe $x=\pm L_x/2$. Current density and temperature profiles in a static filament are shown in the upper panel of Fig. 2. For $\ell_a \gg \ell_T$ the temperature profile essentially follows the current density profile (Fig. 2, curve 1 in the upper panel). For $\ell_a \ll \ell_T$ the characteristic size of the hot area is much larger than the filament size (Fig. 2, curve 2 in the upper panel).

III. MECHANISM OF TRANSLATION INSTABILITY

Antisymmetric (with respect to the center of the filament) fluctuations of the current density do not change the total current and therefore are not suppressed by the external circuit in the current-controlled regime. By increasing the current density on one side and decreasing on another such fluctuation effectively leads to a small shift of a filament, moving one of the filament edges to a cooler region and another to a hotter region. Due to the heat inertia of the semiconductor structure the temperature does not follow the current density instantly. Hence favorable conditions for the impact ionization [production of the activator a in terms of

Eq. (1)] appear at one of the filament edges, whereas at another edge the impact ionization is suppressed. This leads to a further shift of a filament and, for a sufficiently long delay of the temperature response, to a self-sustained filament motion. Experiments[18,21] show that in a high-quality structure filaments start to move to the left and to the right with equal probability. This suggests that motion is triggered by nonequilibrium fluctuations of the current density.

IV. SETTING UP THE STABILITY PROBLEM

A. Linearization and the eigenvalue problem

Let us consider a stationary solution $a_0(x), T_0(x), u_0$ of Eqs. (1)–(3):

$$D_a a_0'' + f(a_0, u_0, T_0) = 0, \tag{5}$$

$$\ell_T^2 T_0'' + \frac{J(a_0,u_0)u_0}{\gamma} - T_0 = 0, \tag{6}$$

$$U_0 - u_0 - RL_y \langle J(a_0,u_0)\rangle = 0. \tag{7}$$

Here the prime $(\cdots)'$ denotes the derivative with respect to x and angular brackets denote integration over the interval $[-L_x/2, L_x/2]$.

Linearization in the vicinity of the stationary solution with respect to the fluctuations

$$a(x,t) - a_0(x) = \delta a(x)\exp(\zeta t),$$

$$u(t) - u_0 = \delta u \exp(\zeta t),$$

$$T(x,t) - T_0(x) = \delta T(x)\exp(\zeta t)$$

leads to the eigenvalue problem

$$\zeta \delta a = \hat{H}_a \delta a + \partial_u f \delta u + \partial_T f \delta T, \tag{8}$$

$$\tau_T \zeta \delta T = \hat{H}_T + \frac{u_0 \partial_a J}{\gamma} \delta a + \frac{J(a_0,u_0) + u_0 \partial_u J}{\gamma} \delta u, \tag{9}$$

$$\tau_u \zeta \delta u = -(1 + RL_y \langle \partial_u J \rangle)\delta u - RL_y \langle \partial_a J \delta a \rangle. \tag{10}$$

Here

$$\hat{H}_a \equiv D_a \frac{d^2}{dx^2} + \partial_a f, \quad \hat{H}_T \equiv \ell_T^2 \frac{d^2}{dx^2} - 1 \tag{11}$$

and all derivatives are computed at the steady–state $a_0(x), T_0(x), u_0$.

B. The reference case $T = T_{\text{ext}}$

Let us briefly summarize the results of the stability analysis in the reference case of constant temperature $T \equiv T_{\text{ext}}$.[35] In this case Eq. (8) is reduced to

$$\zeta \delta a = \hat{H}_a \delta a + \partial_u f \delta u. \tag{12}$$

The eigenfunctions Ψ_i, $i=1, 2, \ldots$, of the self-adjoint operator $\hat{H}_a$ correspond to eigenmodes of the stationary filament in the voltage-controlled regime u=const (Fig. 2, lower panel). These eigenmodes are orthogonal and obey the oscillation theorem which says that Ψ_k has $(k-1)$ nodes inside the interval $[-L_x/2, L_x/2]$. Due to the translation invariance for an infinitely large sample the spectrum of $\hat{H}_a$ contains a neutral (so-called Goldstone) mode

$$\Psi_G \sim a_0' \tag{13}$$

with $\lambda_G = 0$. This mode corresponds to the translation of the filament along the x axis. For a solitary filament $a_0(x)$ has a single maximum. Hence Ψ_G has one node and is identified as Ψ_2.[38] Since $\lambda_2 = 0$ and $\lambda_1 > \lambda_2$, the first eigenvalue λ_1 is positive. The first eigenmode Ψ_1 corresponds to spreading or shrinking of the current filament.

Since a_0 is symmetric with respect to the center of the filament, the "potential term" $\partial_a f$ in the operator $\hat{H}_a$ is also symmetric. Hence Ψ_1 and Ψ_2 are symmetric and antisymmetric, respectively. The increase of Ψ_1 is prevented by the global constraint (3) which effectively fixes the total current when the external resistance R is sufficiently large.[35] In contrast, for $\delta a \equiv \Psi_2$ the last term in the Eq. (10) vanishes due to the asymmetry of Ψ_2. Hence in this case δa and δu are not coupled, and we can take $\delta u = 0$. Physically, it happens because Ψ_2 does not change the total current and therefore the voltage u also does not change. Thus for the current-controlled regime the dynamics of Ψ_2 is the same as in the voltage-controlled regime, and $\zeta = \lambda_2 = 0$.[3,4,35] We conclude that for the two-component model filaments have neutral stability with respect to translation when the lateral dimension of the semiconductor structure is large ($L_x \gg \ell_a$).

C. Translation instability

We shall focus on the second eigenmode Ψ_2 with $\lambda_2 = 0$ and investigate whether for the extended model (1)–(3) the respective increment ζ departs from zero due to the coupling between the master equation (1) and the heat equation (2). As we argued above, in linear approximation the antisymmetric translation mode does not interact with external circuit and hence $\delta u = 0$. The set of equations (8)–(10) reduces to

$$\zeta \delta a = \hat{H}_a \delta a + \partial_T f \delta T, \tag{14}$$

$$\tau_T \zeta \delta T = \hat{H}_T \delta T + (u_0 \partial_a J/\gamma)\delta a. \tag{15}$$

For the model (1)–(3) the translation Goldstone mode $(\delta a_G, \delta T_G)$ has two components which are given by

$$\delta a_G \equiv a_0', \quad \delta T_G \equiv T_0'. \tag{16}$$

By taking the space derivative of Eqs. (5) and (6) we find that $(\delta a_G, \delta T_G)$ indeed satisfies Eqs. (14) and (15) for $\zeta = 0$:

$$\hat{H}_a \delta a_G + \partial_T f \delta T_G = 0, \tag{17}$$

$$\hat{H}_T \delta T_G + (u_0 \partial_a J/\gamma)\delta a_G = 0. \tag{18}$$

V. CHARACTERISTIC EQUATION

The increment ζ of the translation mode can be found from Eqs. (14) and (15) by means of the perturbation theory

with respect to the isothermal case $\zeta=\lambda_2=0$. Substituting $\delta a=\delta a_G$ in Eq. (15) we obtain

$$\tau_T \zeta \delta T = \hat{H}_T \delta T + (u_0 \partial_a J/\gamma)\delta a_G. \tag{19}$$

The solution $\delta T[\zeta,\delta a_G]$ determines the temperature response to the variation δa_G of the activator distribution and depends on both δa_G and ζ. Substitution of $\delta T[\zeta,\delta a_G]$ into Eq. (14) leads to

$$\zeta \delta a_G = \hat{H}_a \delta a_G + \partial_T f \delta T[\zeta,\delta a_G]. \tag{20}$$

Now note that according to Eqs. (18) and (19) δT_G can be presented as

$$\delta T_G \equiv \delta T[\zeta=0,\delta a_G].$$

Therefore according to Eq. (17)

$$\hat{H}_a \delta a_G + \partial_T f \delta T[\zeta=0,\delta a_G] = 0. \tag{21}$$

Substracting Eq. (21) from (20), muliplying by δa_G and integrating over x, we come to the equation for ζ:

$$\zeta = \frac{\langle \partial_T f(\delta T[\zeta,\delta a_G] - \delta T[\zeta=0,\delta a_G]) a_0' \rangle}{\langle (a_0')^2 \rangle}. \tag{22}$$

In the next two sections we find $\delta T[\zeta,\delta a_G]$ and solve Eq. (22) for the limiting cases $\ell_a \gg \ell_T$ and $\ell_a \ll \ell_T$.

VI. WEAK HEAT DIFFUSION

In this section we consider the case $\ell_a \gg \ell_T$ when lateral diffusion of the internal parameter a is much more efficient than the heat diffusion. In this case the temperature profile essentially follows the current density profile (Fig. 2, curve 1 in the upper panel). In the limiting case $\ell_T \to 0$ the solution of Eq. (19) is given by

$$\delta T[\zeta,\delta a_G] = \frac{u_0 \partial_a J}{\gamma(\tau_T \zeta + 1)} \delta a_G. \tag{23}$$

With this input Eq. (22) yields

$$\zeta = \frac{\zeta}{\zeta + \tau_T^{-1}} \Lambda, \quad \Lambda \equiv -\frac{u}{\gamma} \frac{\langle \partial_T f \partial_a J (a_0')^2 \rangle}{\langle (a_0')^2 \rangle}. \tag{24}$$

Two solutions $\zeta=0$ and $\zeta=\Lambda-\tau_T^{-1}$ of this equation appear to intersect at $\tau_T=\Lambda^{-1}$ in the degenerate case ($\lambda_G=0$) under consideration. The relevant branch can be chosen by starting from $\lambda_G \neq 0$ and taking the limit $\lambda_G \to 0$ (see the Appendix). This leads to the piecewise linear dependence

$$\zeta = 0 \text{ for } \tau_T < \Lambda^{-1},$$
$$\zeta = \Lambda - \tau_T^{-1} \text{ for } \tau_T > \Lambda^{-1}. \tag{25}$$

According to Eq. (25), for sufficiently small τ_T the filament remains neutral with respect to translation. The bifurcation from static to traveling filaments occurs with increase of τ_T at $\tau_T=\Lambda^{-1}$.

Note that in the limiting case $\tau_T=0$ the temperature T instantly follows all changes of the current density. In this case T is a local function of the parameter a and can be eliminated by redefining the local kinetic function according to

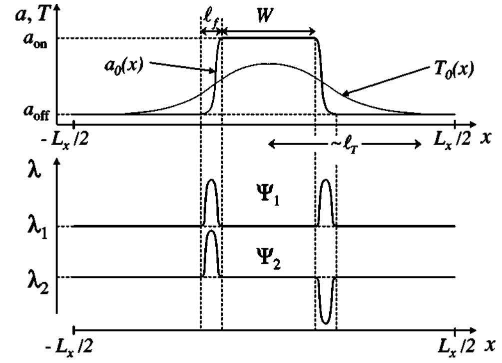

FIG. 3. Profile $a_0(x)$ of the activator and the temperature profile $T_0(x)$ in a wide steady filament (the upper panel). The filament width W, the width of the filament wall ℓ_f and the thermal diffusion length ℓ_T are indicated. Note that in our analysis $L_x \gg W \gg \ell_f$ and $\ell_T \gg \ell_f$, whereas the ℓ_T/W ratio is arbitrary. As in Fig. 2, the low panel sketches two first eigenmodes Ψ_1 and Ψ_2 of the operator $\hat{H}_a$ and their eigenvalues λ_1,λ_2.

$$\tilde{f}(a,u) \equiv f\left(a,u,T=T_{\text{ext}} + \frac{J(a,u)u}{\gamma}\right). \tag{26}$$

In this way the three-component model is reduced back to the two-component model which with respect to the filament stability is equivalent to the isothermal model for $T \equiv T_{\text{ext}}$. Hence for $\tau_T \to 0$ filament has neutral stability, in agreement with Eq. (25). In the opposite case of slow self-heating ($\tau_T=\infty$) the increment ζ has the largest value $\zeta=\Lambda$. Generally, the heat diffusion smoothes the temperature response $\delta T[\zeta,\delta a_G]$, thus shifting the instability threshold to larger values of τ_T.

VII. STRONG HEAT DIFFUSION

In the opposite limiting case $\ell_T \gg \ell_a$ the lateral spreading of heat is more efficient than the lateral spreading of the current density (Fig. 2, curve 2 in the upper pannel). We restrict the analysis to a filament with a flat top (Fig. 3). Such filaments are typical for large structures ($L_x \gg l_a$). The filament width and characteristic width of the filament wall are denoted as W and ℓ_f, respectively. Note that $\ell_f \sim \ell_a$.[34,35]

In this case the translation mode $\Psi_G \sim a_0'$ is distinct from zero only within the filament walls where it has a characteristic value $\pm(a_{\text{on}}-a_{\text{off}})/\ell_f$ (Fig. 3, lower panel). Taking into account the scale separation $\ell_f \ll \ell_T$, we can approximate δa_G as

$$\delta a_G = \sqrt{\ell_f/2}[\delta(-W/2) - \delta(W/2)], \tag{27}$$

where $\delta(x)$ is the delta function, the center of the filament is taken at $x=0$, and the prefactor $\sqrt{\ell_f/2}$ provides normalization $\langle(\delta a_G)^2\rangle=1$. For δa_G given by Eq. (27) the solution $\delta T[\zeta,\delta a_G]$ of Eq. (19) is

$$\delta T = \frac{M\tilde{\ell}_T}{2}\left[1-\exp\left[-\frac{W}{\tilde{\ell}_T}\right]\right]\exp\left(\frac{x+(W/2)}{\tilde{\ell}_T}\right) \text{ for } x<-W/2,$$

$$\delta T = -M\tilde{\ell}_T\exp\left[-\frac{W}{2\tilde{\ell}_T}\right]\sinh\left(\frac{x}{\tilde{\ell}_T}\right) \text{ for } -W/2<x<W/2,$$

$$\delta T = -\frac{M\tilde{\ell}_T}{2}\left[1-\exp\left(-\frac{W}{\tilde{\ell}_T}\right)\right]\exp\left(-\frac{x-(W/2)}{\tilde{\ell}_T}\right) \text{ for } x>W/2, \quad (28)$$

where

$$M(\zeta) \equiv \sqrt{\frac{\ell_f}{2}}\frac{u_0\partial_a J}{\ell_T^2\gamma(1+\tau_T\zeta)}, \quad \tilde{\ell}_T \equiv \frac{\ell_T}{\sqrt{1+\tau_T\zeta}}. \quad (29)$$

Substituting $\delta T[\zeta,\Psi_G)]$ into Eq. (22) we obtain

$$\zeta = \partial_T f\sqrt{\frac{\ell_f}{2}}\left(M(\zeta)\tilde{\ell}_T(\zeta)\left[1-\exp\left(-\frac{W}{\tilde{\ell}_T(\zeta)}\right)\right] - M(0)\ell_T\left[1-\exp\left(-\frac{W}{\ell_T}\right)\right]\right). \quad (30)$$

Taking into account that near the bifurcation point ζ is small, we expand the right-hand side of Eq. (30) over $(\tau_T\zeta)$ and come to the equation

$$\zeta = \Omega\frac{\tau_T\zeta}{2+\tau_T\zeta}, \quad \Omega \equiv \frac{\ell_f}{\ell_T}\frac{u_0\partial_T f\partial_a J}{2\gamma}A(W),$$
$$A(W) \equiv 1-\left(1+\frac{W}{\ell_T}\right)\exp\left(-\frac{W}{\ell_T}\right). \quad (31)$$

Equation (31) coincides with Eq. (24) when Λ is replaced by Ω and τ_T by $(\tau_T/2)$. Hence the solutions have the same structure as in Eq. (25):

$$\zeta = 0 \text{ for } \tau_T < 2\Omega^{-1},$$
$$\zeta = \Omega - 2\tau_T^{-1} \text{ for } \tau_T > 2\Omega^{-1}. \quad (32)$$

VIII. DISCUSSION

A. Onset of filament motion for weak and strong heat diffusion

For $\ell_T \ll \ell_a$ the condition for the onset of filament motion is given by Eq. (25) and can be presented as

$$\tau_T > \tau_1^{\text{th}} \equiv \Lambda^{-1} = \frac{\gamma}{u_0}\frac{\langle(a_0')^2\rangle}{\langle\partial_T f\partial_a J(a_0')^2\rangle}. \quad (33)$$

In the opposite limiting case $\ell_T \gg \ell_a$ this condition is given by

$$\tau_T > \tau_2^{\text{th}} \equiv \frac{4\ell_T}{\ell_f A(W)}\frac{\gamma}{u_0\partial_T f\partial_a J}. \quad (34)$$

In both cases $\ell_a \ll \ell_T$ and $\ell_a \gg \ell_T$ the instability occurs when the thermal relaxation time τ_T is sufficiently large. This suggests that τ_T is a bifurcation parameter also in the intermediate case $\ell_a \sim \ell_T$.

The relation between τ_1^{th} and τ_2^{th} becomes transparent when $\partial_T f$ and $\partial_a J$ are considered as constants. (Note also that $\ell_f \sim \ell_a$.) In this case

$$\tau_2^{\text{th}} \sim \frac{4\ell_T}{\ell_a A(W)}\tau_1^{\text{th}}. \quad (35)$$

For wide ($W \gg \ell_T$) and narrow ($W \ll \ell_T$) filaments the expansion of $A(W)$ over W/ℓ_T [see Eq. (31)] leads to

$$\tau_2^{\text{th}} \sim \frac{\ell_T}{\ell_a}\tau_1^{\text{th}} \text{ for } W \gg \ell_T,$$
$$\tau_2^{\text{th}} \sim \frac{2(\ell_T)^3}{\ell_a W^2}\tau_1^{\text{th}} \text{ for } W \ll \ell_T. \quad (36)$$

Thus the threshold time τ_2^{th} exceeds τ_1^{th} by a factor which is always larger than ℓ_T/ℓ_a.

For $\ell_T \gg \ell_a$ the instability threshold has been previously obtained in Ref. 22 for the current density profile as shown in Fig. 3. The argument is based on the finding that the velocity v of the stationary filament motion is proportional to the difference of temperatures at the front and back filament edges ΔT: $v = C\Delta T$.[22] This temperature difference, in turn, depends on the v. Hence the velocity of stationary motion can be found from the equation $v = C\Delta T(v)$. Since for $v=0$ the temperature profile is symmetric, $\Delta T(0)=0$. Therefore $v=0$ is always a solution of this equation. However, this solution is unstable if $\Delta T(v)$ increases faster than v/C with increase of v. In this case when v deviates from $v=0$, the "overproduction" of the the temperature difference ΔT leads to further increase of v. The respective condition is given by[22]

$$\frac{v_0}{2v_T}A(W) > 1, \quad v_0 \equiv \frac{(J_{\text{on}}-J_{\text{off}})u_0}{\gamma\langle(a_0')^2\rangle}\int_{a_{\text{off}}}^{a_{\text{on}}}\partial_T f da. \quad (37)$$

Here v_0 has the meaning of the upper limit of the filament velocity and $v_T \equiv \ell_T/\tau_T$ is the thermal velocity. $J_{\text{on}}, J_{\text{off}}$ and a_{off}, a_{on} are the current denisties and the values of the variable a corresponding to the uniform on and off states at $u = u_0$, respectively (Fig. 3). $A(W)$ is exactly the same as in Eq. (30). The criterium (37) can be rewritten as

$$\tau_T > \tilde{\tau}_2^{\text{th}}, \quad \tilde{\tau}_2^{\text{th}} = \frac{2}{A(W)}\frac{\ell_T}{v_0}. \quad (38)$$

Taking into account that for a wide filament

$$\langle(a_0')^2\rangle \approx 2(a_{\text{on}}-a_{\text{off}})^2/\ell_f \quad (39)$$

and considering the function $\partial_T f$ as a constant, we find

$$v_0 \approx -\frac{\partial_T f u_0}{2\gamma}\frac{J_{\text{on}}-J_{\text{off}}}{a_{\text{on}}-a_{\text{off}}}. \quad (40)$$

Hence

$$\tilde{\tau}_2^{\text{th}} = \frac{4\ell_T}{\ell_f A(W)} \frac{\gamma}{u_0 \partial_T f} \frac{a_{\text{on}} - a_{\text{off}}}{J_{\text{on}} - J_{\text{off}}}. \tag{41}$$

Comparing Eqs. (34) and (41), we see that $\tilde{\tau}_2^{\text{th}}$ coincides with τ_2^{th} [see Eq. (34)] if we approximate the partial derivative $\partial_a J$ by the finite difference

$$\partial_a J \sim (J_{\text{on}} - J_{\text{off}})/(a_{\text{on}} - a_{\text{off}}).$$

B. Traveling filament

Remarkably, the difference between the regimes of weak and strong heat diffusion, which is well pronounced near the bifurcation from static to traveling filament, vanishes for fast self-sustained filament motion with velocity $v \gg v_T$. In this regime the static thermal diffusion length $\ell_T = \sqrt{D_T \tau_T}$ should be replaced by $\mathcal{L}_T = \sqrt{D_T \tau_f}$, where $\tau_f = W/v$ is the time of the filament passage over its width W and $D_T = \kappa / c\rho$ is thermal diffusivity. For $\mathcal{L}_T \ll W$ the heat diffusion is negligible. This condition yields

$$v \gg D_T/W = v_T \ell_T / W. \tag{42}$$

For typical filament width $W \sim 10$ μm the condition (42) yields $v \gg 10^3$ cm/s for Si and $v \gg 250$ cm/s for GaAs ($D_T = 0.92$ and 0.25 cm^2/s, respectively).

If the condition $\mathcal{L}_T \ll W$ is met together with the condition $\tau_f \ll \tau_T$, the heating is not only local but also adiabatic. (Note that for $\ell_T \sim W$ these two conditions are equivalent.) In this case the rate of temperature increase in each point is proportional to the local power dissipation. The velocity of such fast narrow filament has been obtained in Ref. 22:

$$v \approx \sqrt{v_0 W / \tau_T}. \tag{43}$$

Substituting the definitions τ_T and v_0 [see Eqs. (4) and (40)], we find that the filament velocity is proportional to the square root of the total Joule power which is dissipated in the filament:

$$v = \sqrt{\frac{KP}{c\rho}}, \quad P \equiv \frac{(J_{\text{on}} - J_{\text{off}}) W u_0}{w} \approx \frac{J_{\text{on}} W u_0}{w}, \tag{44}$$

where $c\rho$ is specific heat per unit volume and the coefficient K is given by

$$K \equiv \frac{1}{\langle (a_0')^2 \rangle} \int_{a_{\text{off}}}^{a_{\text{on}}} \partial_T f da \sim \frac{\ell_f \partial_T f}{2(a_{\text{on}} - a_{\text{off}})^2}. \tag{45}$$

Alternative elementary derivation of the square root dependence is presented in Ref. 21.

Apparently, the square root dependences (43) and (44) reflect the experimental situation which is favorable for observation of traveling filaments because large velocity corresponds to low instability threshold. It has been reported[21] that the results of experimental measurements of the filament velocity in a Si device ($v \sim 3 \times 10^4$ cm/s, $W \sim 10$ μm) indeed obey the square root dependence.

C. The type of bifurcation

The piecewise linear dependence (25) and (32) of the increment ζ on the bifurcation parameter τ_T^{-1} as well as the square root behavior of the filament velocity near the bifurcation point, predicted in Ref. 22, are qualitatively the same as obtained in Ref. 26 for the three-component "cubic" model for a traveling spot. These features seem to be typical for a degenerate "drift pitchfork" bifurcation associated with $\lambda_G = 0$. Note that the mechanism of self-motion described here for one-dimensional spatial domains is also valid for two-dimensional domains. The difference between the model (1)–(3) and three-component models for traveling spots studied in Refs. 23–27 has been discussed in Ref. 22.

D. The alternative mechanism for self-motion of a current filament

Generally, the self-motion of a current filament becomes possible when a semiconductor structure, apart from the activator mechanism which leads to bistability, posseses an internal mechanism of slow inhibition. As we described here, such mechanim can appear due to the effect of Joule heating on the cathode–anode electron transport. Another inhibitor mechanism of purely electrical origin has been discussed in Refs. 16 and 39–41. For this mechanism inhibition is associated with the internal voltage drop across the plasma layer inside the semiconductor structure. The regions of activation and inhibition are spatially separated. The effective reaction–diffusion model[16,42,43] for such two-layer system has the same structure as Eqs. (1)–(3). Recent numerical simulations demonstrate that this mechanism leads to filament motion during the switching-off transients in power diodes.[41] The applicability of this concept to thyristorlike $p^+ - n^+ - p - n^- - n^+$ structures discussed in Ref. 16 should be considered in view of the latest studies[44–46] which reveal complexity of the vertical transport processes in these multilayer structures.

IX. CONCLUSIONS

Joule self-heating of a static current-density filament may lead to the translation instability and the onset of thermally driven self-motion. This may occur in a wide class of semiconductor devices whose bistability is caused by impact ionization because impact ionization coefficients decrease with temperature. The eigenvalue of the respective translation mode, which is zero when heating is neglected, becomes positive due to the suppressive effect of temperature on the electron transport in the cathode–anode direction. Increments of the translation mode are found for the limiting cases of weak (25) and strong (32) heat diffusion. In both cases the instability threshold (33) and (34) is controlled by the thermal relaxation time τ_T and is directly proportional to $\partial_T f$. It scales as ℓ_T / ℓ_a with increase of the thermal diffusion length ℓ_T.

ACKNOWLEDGMENTS

The author is grateful to A. Alekseev for critical reading of the manuscript and the hospitality at the mathematical department of the University of Geneva and to D. Pogany for helpful discussions. This work has been supported by the Swiss National Science Foundation.

APPENDIX: INCREMENT OF THE TRANSLATION MODE

To indentify the physical branch of the solution of Eq. (24), we note that for $\lambda_G \neq 0$ this equation becomes

$$\zeta = \lambda_G + \frac{\zeta}{\zeta + \tau_T^{-1}}\Lambda. \quad \text{(A1)}$$

Smooth solution of this quadratic equation

$$\zeta = \frac{\lambda_G + \Lambda - \tau_T^{-1}}{2} + \sqrt{\frac{(\lambda_G + \Lambda - \tau_T^{-1})^2}{4} + \frac{\lambda_G}{\tau_T}} \quad \text{(A2)}$$

for $\lambda_G \to 0$ tends to the piecewise linear dependence given by Eq. (25). Note the similarity of Eqs. (A1) and (A2) and Eq. (9) in Ref. 25.

*Electronic address: rodin@mail.ioffe.ru

[1] A. L. Zakharov, Zh. Eksp. Teor. Fiz. **38**, 665 (1960) [Sov. Phys. JETP **11**, 479 (1960)].

[2] B. K. Ridley, Proc. Phys. Soc. London **82**, 954 (1963).

[3] A. F. Volkov and Sh. M. Kogan, Zh. Eksp. Teor. Fiz. **52**, 1647 (1967) [Sov. Phys. JETP **25**, 1095 (1967)]; Usp. Fiz. Nauk **96**, 633 (1968) [Sov. Phys. Usp. **11**, 881 (1969)].

[4] F. G. Bass, V. S. Bochkov, and Yu. Gurevich, Zh. Eksp. Teor. Fiz. **58**, 1814 (1970) [Sov. Phys. JETP **31**, 972 (1970)].

[5] I. V. Varlamov, V. V. Osipov, and E. A. Poltoratsky, Fiz. Tekh. Poluprovodn. (S.-Peterburg) **3**, 1162 (1969) [Sov. Phys. Semicond. **3**, 978 (1970)].

[6] V. V. Osipov and V. A. Kholodnov, Fiz. Tekh. Poluprovodn. (S.-Peterburg) **4**, 1216 (1970) [Sov. Phys. Semicond. **4**, 1033 (1971)].

[7] V. V. Osipov and V. A. Kholodnov, Mikroelektronika **2**, 529 (1973).

[8] V. L. Bonch-Bruevich, I. P. Zvyagin, and A. G. Mironov, *Domain Electrical Instabilities in Semiconductors* (Consultant Bureau, New York, 1975).

[9] E. Schöll, *Nonequilibrium Phase Transitions in Semiconductors* (Springer-Verlag, Berlin, 1987).

[10] A. Wacker and E. Schöll, Z. Phys. B: Condens. Matter **93**, 431 (1994).

[11] F.-J. Niedernostheide, H. J Schulze, S. Bose, A. Wacker, and E. Schöll, Phys. Rev. E **54**, 1253 (1996).

[12] B. Datsko, Fiz. Tekh. Poluprovodn. (S.-Peterburg) **11**, 250 (1996) [Semiconductors **31**, 146 (1997)].

[13] S. Bose, P. Rodin, and E. Schöll, Phys. Rev. E **62**, 1778 (2000).

[14] K. Penner, J. Phys. Colloq. C4 **49**(9), 797 (1988).

[15] G. Wachutka, IEEE Trans. Electron Devices **38**, 1516 (1991).

[16] F.-J. Niedernostheide, B. S. Kerner, and H.-G. Purwins, Phys. Rev. B **46**, 7559 (1992).

[17] D. Pogany, S. Bychikhin, M. Litzenberger, E. Gornik, G. Groos, and M. Stecher, Appl. Phys. Lett. **81**, 2881 (2002).

[18] D. Pogany, S. Bychikhin, E. Gornik, M. Denison, N. Jensen, G. Groos, and M. Stecher, *Moving Current Filaments in ESD Protection Devices and their Relation to Electrical Characteristics*, Proceedings of the IEEE Reliability Physics Symposium, IRPS2003, Dallas, Texas, 2003 (Electron Device Society and the Reliability Society of the Institute of Electrical and Electronics Engineers, Inc., 2003), pp. 241–248.

[19] R. Steinhoff, J.-B. Huang, P. L. Hower, and J. S. Brodsky, *Current Filament Movement and Silicon Melting in an ESD-Robust DENMOS Transistor*, Proceedings of the Electrical Overstress/Electrostatic Discharge Symposium, Las Vegas, 2003, pp. 7–16.

[20] M. Denison, M. Blaho, P. Rodin, D. Pogany, D. Silber, E. Gornik, and M. Stecher, IEEE Trans. Electron Devices **58**, 1331 (2004).

[21] D. Pogany, S. Buchikhin, M. Denison, P. Rodin, N. Jensen, G. Groos, M. Stecher, and E. Gornik, Solid-State Electron. (to be published).

[22] P. Rodin, Phys. Rev. B **69**, 045307 (2004).

[23] K. Krischer and A. Mikhailov, Phys. Rev. Lett. **73**, 3165 (1994).

[24] A. N. Zaikin, Fiz. Mysl' Rossii **1**, 54 (1995).

[25] C. P. Schenk, M. Or-Guil, M. Bode, and H.-G. Purwins, Phys. Rev. Lett. **78**, 3781 (1997).

[26] M. Or-Guil, M. Bode, C. P. Schenk, and H.-G. Purwins, Phys. Rev. E **57**, 6432 (1998).

[27] M. Bode, A. W. Liehr, C. P. Schenk, and H.-G. Purwins, Physica D **161**, 45 (2002).

[28] A. S. Mikhailov and V. Calenbuhr, *From Cells to Societies: Models of Complex Coherent Action*, Springer Series in Synergetics (Springer, Berlin, 2002).

[29] E. Mihaliuk, T. Sakurai, F. Chirila, and K. Showalter, Phys. Rev. E **65**, 065602(R) (2002).

[30] T. Sakurai, E. Mihaliuk, F. Chirila, and K. Showalter, Science **296**, 1917 (2002).

[31] K. G. McKay, Phys. Rev. **94**, 877 (1954).

[32] S. M. Sze, *Physics of Semiconductor Devices* (Wiley, New York, 1981).

[33] E. Schöll, *Nonlinear Spatio-Temporal Dynamics and Chaos in Semiconductors* (Cambridge University Press, Cambridge, U.K., 2001).

[34] A. Wacker and E. Schöll, J. Appl. Phys. **78**, 7352 (1995).

[35] A. Alekseev, S. Bose, P. Rodin, and E. Schöll, Phys. Rev. E **57**, 2640 (1998).

[36] M. Meixner, P. Rodin, E. Schöll, and A. Wacker, Eur. Phys. J. B **13**, 157 (2000).

[37] The opposite case $\partial_T f > 0$ corresponds to the positive temperature effect and occurs, e.g., when thermogeneration sets in (Ref. 22).

[38] Note that for Neumann boundary conditions imposed on the activator a, the functions Ψ_2 and Ψ_G satisfy Neumann and Dirichlet boundary conditions, respectively, and therefore do not exactly coincide (Ref. 35). This difference becomes important when L_x is comparable to the filament size. Then the eigenvalue λ_2 becomes positive refelecting the attractive effect of boundaries on the filament. This effect decreases exponentially with L_x and is not considered here.

[39] *Nonlinear Dynamics and Pattern Formation in Semiconductors and Devices*, edited by F.-J. Niedernostheide (Springer-Verlag, Berlin, 1995).

[40] F.-J. Niedernostheide, M. Or-Guil, M. Kleinkes, and H.-G. Purwins, Phys. Rev. E **55**, 4107 (1997).

[41] F.-J. Niednostheide and H.-J. Schulze, Physica D **199**, 129 (2004).
[42] Ch. Radehaus, K. Kardell, H. Baumann, D. Jäger, and H.-G. Purwins, Z. Phys. B: Condens. Matter **65**, 515 (1987).
[43] B. S. Kerner and V. V. Osipov, *Autosolitons* (Kluwer Academic, Dordrecht, 1994).
[44] A. Wierschem, F.-J. Niedernostheide, A. Gorbatyuk, and H.-G. Purwins, Scanning **17**, 106 (1995).
[45] A. V. Gorbatyuk and F.-J. Niedernostheide, Physica D **99**, 339 (1996).
[46] A. V. Gorbatyuk and F.-J. Niedernostheide, Phys. Rev. B **59**, 13 157 (1999); **65**, 245318 (2002).